A comparison of Landsat-8 and Sentinel-2 spectral indices for estimating aboveground forest carbon in a community forest

Anish KC[1]*, Sanjeeb Bhattarai[1] and Pravesh Pandey[1]

[1] *Institute of Forestry, Hetauda Campus, Hetauda, Nepal*

ABSTRACT

This study aimed to estimate and map the Above Ground Forest Carbon stock in the Salbote Karele Community Forest in Ilam district. The research used field surveys and satellite data from Sentinel-2 and Landsat-8 to determine biomass and carbon stocks. A total of 30 inventory plots covering 283.56 hectares (ha) were surveyed, resulting in an estimated mean biomass of 156.48 ton ha^{-1} and carbon stock of 73.55 ton ha^{-1}. The biomass was then correlated with five different Vegetation Indices (VIs), computed from Sentinel-2 and Landsat-8 image and used to develop various simple linear regression models. The study found that Sentinel-2 data showed the highest correlation with observed biomass (R^2 = 0.76) and lowest prediction error (RMSE = 78.44 tonha-1) compared to Landsat-8 data. The linear regression model developed from Sentinel-2's NDVI (Normalized Difference Vegetation Index) data predicted a mean AGB of 129.82 ton ha^{-1} and AGC of 61.01 ton ha^{-1}. This research highlights the importance of using Sentinel-2 data for estimating Above Ground Forest Carbon stocks due to its combination of spectral capabilities and broad applicability. It also shows that the Salbote Karele community forest is of great significance as it stores suitable amounts of carbon.

Introduction

Forest ecosystems are among the world's greatest terrestrial carbon storages and contribute significantly to the global carbon cycle. Forest ecosystem carbon pools comprise above-ground biomass (AGB), below-ground biomass, deadwood, litter, and peat soil (IPCC, 2006). Of these, AGB contains the largest carbon pool and is most directly impacted by deforestation and forest degradation. Estimating AGB is the primary step in quantifying the carbon stock of a forest as dry biomass contains about 47% carbon (IPCC, 2006). Nepal is a developing

country with a forest cover of about 6.16 million hectares (ha) or 41.69% of the total geographical area of the country (FRTC, 2022). Community forestry is the top priority programme for the forestry sector in the country. About 3.18 million of forest (48.12% of total forest in the country) are managed by community-based forest management (MoFE, 2020). The REDD+ (Reducing Emissions from Deforestation and Degradation) scheme for developing countries aims to reduce emissions from forested lands and invest in sustainable development by providing a financial value according to the quantity of carbon stored in forests (Asner et al., 2012; FAO, 2010). With forests occupying more than 40 percent of its territory, Nepal is an important target for REDD+ projects. (Hussin and Gilani, 2011). The accuracy of AGB estimation is key to understanding trends in the carbon flux. This is useful in addressing problems of deforestation and degradation and gaining carbon mitigation benefits through mechanisms such as REDD+ (Hussin et al., 2011; Kim et al., 2010; Lu DS, 2006). Furthermore, evaluation of AGB offers insights for managers, forestry professionals and scientists in understanding the impact of ecosystem changes on the global carbon cycle, tracking the effects of climate change, and accurately measuring the amount of carbon stored in the land (Chinembiri et al., 2013; Gara et al., 2014; Lu DS, 2006). Additionally, regular forest monitoring informs planning strategies and decision-making for responsible utilization of forest resources and conservation.

Forest AGB is generally estimated through a traditional field inventory. There is no doubt that traditional methods are more accurate, but they are also time-consuming, laborious and difficult to implement in inaccessible and large areas (Lu DS, 2006; Henry et al., 2011). Remote sensing provides a consistent and dependable alternative for a more robust, continuous, and spatially explicit biomass assessment (Herold et al., 2007). It has been demonstrated in several studies that satellite spectral information correlates strong with aboveground forest biomass and when combined with field measurements is a suitable estimation for AGB (Viana et al., 2012; Lu et al., 2012 ; Manna et al., 2014 ; Kushwaha et al., 2014)

In the past three decades, Landsat images have predominantly been utilized for estimating forest AGB (Dube et al., 2015; Hall et al., 2006; Powell et al., 2009) due to their widely available long-term archive images with moderate spatial resolution. However, a common challenge is data saturation in Landsat imagery, where an increase in biomass leads to spectral saturation and ultimately results in under-estimation of biomass. For example, a study by Kasischke et al. (2015) found that significant differences in the accuracy of biomass and VIs were caused by the saturation of spectral indices at higher biomass values. Achieving accurate AGB estimation in complex sub-tropical regions such as Nepal requires high-resolution data, particularly if the goal is to overcome the saturation problem. Sentinel-2 is a state-of-the-art sensor with wide spatial coverage and high spatial and temporal resolution. It offers high resolution imagery, with four bands at 10-meter resolution (Blue-Band 2, Green-Band 3, Red-Band 4, NIR-Band 8) and one band at 20-meter resolution (NIR-Band 8A).These bands cover a major portion of vegetation absorption and reflectance behaviour and demonstrate a strong relationship with forest attributes (Barati et al., 2011).

Although several studies have been conducted on the use of remote sensing data in tropical forests, only a few have combined different techniques involving field estimation to quantify the forest biomass (Næsset et al., 2016). Previous studies have mainly concentrated on using Sentinel-2 for determining the chlorophyll and nitrogen content of grasses (Clevers et al., 2013), evaluating the quality of rangelands (Ramoelo et al., 2015), mapping and monitoring wetlands (Kaplan and Avdan, 2017) and tree canopy cover (Godinho et al., 2017). However, the capability of using VIs to estimate and map AGB has not been thoroughly investigated, and only a limited number of

studies have been conducted on its ability to estimate forest biomass, particularly in the case of community forests in Nepal. In such areas, the use of Sentinel-2, with its high-resolution imagery and open access policy, could offer new opportunities for accurate and prompt estimation of biomass.

This study of a community forest in Ilam district represents a significant opportunity to advance our understanding of the application of remote sensing techniques to estimate above-ground forest carbon across the challenging topographic landscapes such as the Churia region of Nepal. This study aims to contribute to a growing body of literature in this field by evaluating the efficacy of utilizing freely accessible satellite imagery, including Landsat and Sentinel, for estimating forest carbon. The results of this study have the potential to inform the development of more comprehensive remote sensing-based approaches for monitoring above-ground forest carbon and support the implementation of sustainable forest management practices. The objectives of the study are (1) to estimate biomass and carbon storage in community forest area through field inventory, (2) to compare various Sentinel-2 indices with Landsat-8-derived indices and (3) to prepare the biomass and carbon stock map of the study area using best fit regression modelling.

Materials and Methods

Study area
This study is conducted in Salbote Karele community forest (C.F) of Ilam district (Figure 1). Extending over an area of 1,703 sq km, Ilam is a hilly district situated about 600 km east from Kathmandu, in Province No. 1 of Nepal.
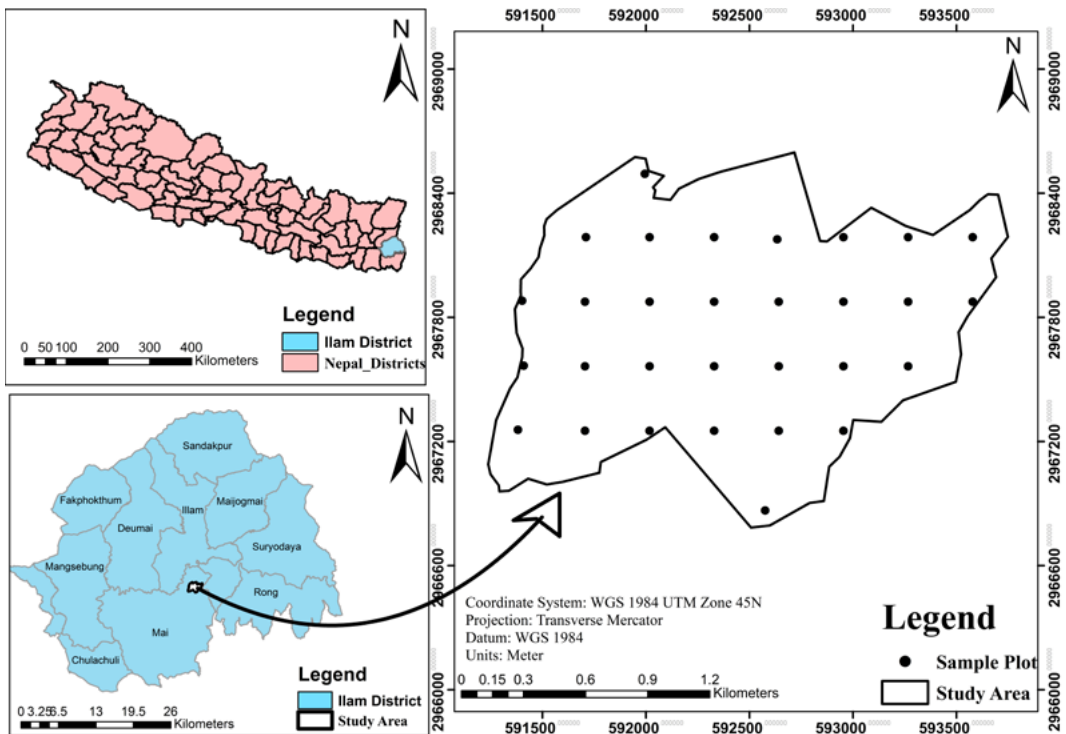
Figure 1 :Location map of the study area

It is located between 260 40' – 270 08' N latitudes and 870 40' – 880 10' E longitudes. The district stretches across the lower belt of the Terai (flat land stretching all along the southern border with India) and Chure (a stretch of Siwalik hills extending from east to west on the north, next to the Terai) and into the upper hilly belt of the Himalayan region with total altitude ranging from 150 m to 3,636 m above mean sea level (amsl) (Bhattarai et al., 2016). Tropical to alpine vegetation is found in the district, with total forest coverage of c. 55% of the total area (FRA, 2015). SalboteKarele CF is situated in Mai Municipality-10 of Ilam district. Mai Municipality has forest cover of 61.1% (DFRS, 2018).This community forest is moderately dense in the southern Chure region of Ilam district and covers an area of 283.56 ha. The major tree species found in this community forest include *Shorea robusta, Terminalia tomentosa, Schima wallichi, Bombax ceiba, Terminalia chebula, Lagerstroemia parviflora, Adina cordifolia.*

Forest inventory

For field data collection, a systematic sampling approach was used in conjunction with circular sample plots of 500 m^2 (12.62 m radius). The number of field sample plots required was calculated using an equation from Husch et al. (2003).

$$N = \frac{t^2 * CV^2}{AE\%^2}$$

where, N is the number of sample plots, t is the statistical value at 95% significance level, CV is the coefficient of variation of DBH (Diameter at Breast Height) of the trees to be sampled, and AE is the allowable error for DBH of trees to be sampled.

From the available secondary data received from the operational plan of the CF, a CV of 42.7 and a t-value of 1.19 were obtained at 95% confidence level. Keeping 10% of allowable error for the DBH of trees to be sampled, the minimum number of sample plots required was

26.

Thirty systematically distributed field plots were measured and recorded. The methodology for each plot sample included species name, the DBH at 1.37 m above ground, and the height of all trees with DBH ≥ 10cm.

Forest Above Ground Biomass Estimation (FAGB):

The allometric equation formulated by Chave et al. (2014) was used in this research. It was found to be the best fit pan-tropic model for biomass estimation. It is also suitable for all forest types and bioclimatic conditions.

$$FAGB = 0.0673 * (\rho * D2 * H)0.976$$

Where,
   ρ = Specific wood density (g/cm^3)
   D= Diameter at breast height (DBH) (cm)
   H= Height of tree (m)

The specific wood density values of tree species were derived from Sharma and Pukkala (1990) Forest Above Ground Carbon Stock Estimation (FAGC):

The calculated above-ground biomass was converted into carbon using the (CF) factor 0.47 formulated by IPCC (2006).

$$\text{i.e. FAGC = AGB x CF}$$

Remote sensing dataset and pre-processing

Single tile standard Sentinel-2 and Landsat 8 product, cloud-free (<10% cloud cover) images close to the field inventory date were downloaded from the Copernicus Sentinel Scientific Data Hub (*https://scihub.copernicus.eu/*) and USGS (United States Geological Survey) Earth Explorer (*https://earthexplorer.usgs.gov*) respectively, which are open-source websites. The specifications of satellite imagery are listed in Table 1.

The acquired Landsat-8 data set was a high-level product that was already processed

to calibrate raw digital numbers (DNs) to Top of the Atmosphere (TOA) reflectance and then corrected to surface reflectance using atmospheric parameters and Digital Elevation Model (DEM). Furthermore, TOA brightness temperature and masks for clouds, cloud shadows, adjacent clouds, land, and water were also already available as high-level products from the USGS (Palareti et al., 2016). Therefore, for atmospheric correction, only sun angle correction has been applied. The Semi-automatic Classification plugin in QGIS 3.8.2 was utilized to transform radiance imagery to surface reflectance through Dark Object Subtraction (DOS). The DOS technique operates by eliminating the darkest pixel in each band, which is impacted by atmospheric scattering (Chavez Jr, 1988). The red and near-infrared bands of the Sentinel and Landsat data were used as they have been widely accepted for vegetation monitoring and biomass estimates. The five VIs, which included NDVI, SAVI, DVI, MSAVI, and EVI, were calculated using the equations in Table 2.

Table 1: Satellite images used for calculating vegetation indices

S.N	Satellite Images	Number of bands	Spatial Resolution (m)	Cloud cover (%)
1	Landsat-8	2, 4, 5	30 m	Less than 2
2	Sentinel-2	2, 4, 8	10 m	Less than 2

Correlation analysis

AGB shape file created via QGIS 3.8.2 was overlain on corresponding VIs of both the acquired images. The values of masked pixels by inventory plots were extracted for all the indices. A correlation analysis between the field estimated biomass and extracted pixel values of each vegetation index was done to understand the association between biomass and the VIs. Pearson's correlation analysis was applied and the significance of the relationship was also assessed using the P-Value, for which a value of< 0.05 was considered significant.

Model development for biomass estimates and validation

Based on the correlation between the VIs and field measured biomass, a simple linear model was established for each satellite data set. From the field inventory data, 70% of the data set was used for model estimation while the remaining 30% was for evaluating the model performance (validation). Each model was assessed by coefficient of determination (R^2) and significant value (P-value) and Root Mean Square Error (RMSE). The final model for biomass estimation and mapping was taken, which has the highest coefficient of determination (R^2), least P-value and least RMSE. The predicted data for each model were taken as the independent variable and observed as the dependent following recommendation from Piñeiro et al. (2008).

Table 2: List and Formulas for different vegetation indices

Vegetation indices (VIs)	Formula	Sentinel-2	Landsat-8
Normalized Difference Vegetation Index (NDVI)	$\dfrac{(NIR - R)}{(NIR + R)}$	$\dfrac{(B8 - B4)}{(B8 + B4)}$	$\dfrac{(B5 - B4)}{(B5 + B4)}$
Soil Adjusted Vegetation Index (SAVI)	$\dfrac{(NIR - R)}{(NIR + R + L)} * (1 + L)$	$\dfrac{(B8 - B4)}{(B8 + B4 + 0.5)} * (1 + 0.5)$	$\dfrac{(B5 - B4)}{(B5 + B4 + 0.5)} * (1 + 0.5)$
Difference Vegetation Index (DVI)	$NIR - R$	$B8 - B4$	$B5 - B4$
Modified Soil Adjusted VegetationIndex (MSAVI)	$\dfrac{2NIR + 1 - \sqrt{(2NIR + 1)^2 - 8(NIR - R)}}{2}$	$\dfrac{2B8 + 1 - \sqrt{(2B8 + 1)^2 - 8(B8 - B4)}}{2}$	$\dfrac{2B5 + 1 - \sqrt{(2B5 + 1)^2 - 8(B5 - B4)}}{2}$
Enhanced vegetation index (EVI)	$2.5 * \dfrac{(NIR - R)}{NIR + 6 * R - 7.5 * B + 1}$	$2.5 * \dfrac{(B8 - B4)}{B8 + 6 * B4 - 7.5 * B2 + 1}$	$2.5 * \dfrac{(B5 - B4)}{B5 + 6 * B4 - 7.5 * B2 + 1}$

Here, L=soil brightness correction factor i.e. 0.5

Results and Discussion

Biomass and carbon stock from field inventory
The major forest tree species found in the study area were *Shorea robusta, Terminalia tomentosa, Schima wallichi, Bombax ceiba,* and *Terminalia chebula.* Table 3 shows Biomass and Carbon stock estimated per plot calculated from the field inventory data collected from 30 plots in the study area. The AGB ranged from 16.60 ton ha^{-1} to 497.59 ton ha^{-1} with the mean of 156.48 ton ha^{-1}. The above ground carbon (AGC) ranged from 7.80 ton ha^{-1} to 233.87 ton ha^{-1} with the mean of 73.55 ton ha^{-1}. Total AGB in the study area was 44372.95 ton and total AGC in the study area was 20855.29 ton.

According to IPCC, the range of AGB in tropical forest in Asia is about 67.7 ton ha^{-1} to 184.6 ton ha^{-1}(Rozendaal et al., 2022) and, according to Subedi et al. (2022), the average estimated AGC for the Churia region of Nepal was 89.20 ton ha^{-1}. which is higher than the estimates from the current study. This higher average may reflect the study area being only a moderately dense forest that has also been affected by encroachment in different parts for settlement.

Table 3: Biomass and carbon stocks of the sample plots

Plot No.	Forest Above Ground Biomass (kg)	Forest Above Ground Biomass (ton ha^{-1})	Forest Above Ground Carbon (ton ha^{-1})
1	14253.65	285.07	133.98
2	9310.91	186.22	87.52
3	2273.20	45.46	21.37
4	9109.91	182.20	85.63
5	2413.22	48.26	22.68
6	2970.72	59.41	27.92
7	5475.65	109.51	51.47
8	8990.30	179.81	84.51
9	14157.67	283.15	133.08
10	5224.90	104.50	49.11
11	11866.51	237.33	111.55
12	7853.15	157.06	73.82
13	8546.55	170.93	80.34
14	24879.56	497.59	233.87
15	4631.67	92.63	43.54
16	2587.82	51.76	24.33
17	829.99	16.60	7.80
18	9675.16	193.50	90.95
19	7464.38	149.29	70.17
20	6593.66	131.87	61.98
21	7240.23	144.80	68.06
22	17154.28	343.09	161.25
23	4483.08	89.66	42.14
24	3318.41	66.37	31.19
25	4524.85	90.50	42.53
26	12366.13	247.32	116.24
27	8675.12	173.50	81.55
28	3339.92	66.80	31.40
29	7663.02	153.26	72.03
30	6854.24	137.08	64.43
Average		**156.49**	**73.55**

Correlation analysis

The correlation coefficients for different VIs calculated from both the Landsat-8 and sentinel-2 are presented in Table 4 and Table 5 respectively and represented in scatter plot graphs in Figure 2 and Figure 3 respectively. All VIs from both the satellites were observed to correlate positively with the estimated field biomass. Thus, the study detected significant correlation of ($r = 0.708$, $p < 0.001$) for NDVI, ($r = 0.380$, $p < 0.01$) for DVI, ($r = 0.593$, $p < 0.001$) for MSAVI, ($r = 0.614$, $p < 0.001$) for SAVI, ($r = 0.453$, $p < 0.01$) for EVI calculated from Landsat-8 imagery and similarly significant correlation of ($r = 0.797$, $p < 0.001$) for NDVI,($r = 0.455$, $p < 0.01$) for DVI, ($r = 0.532$, $p < 0.001$) for MSAVI, ($r = 0.594$, $p < 0.001$) for SAVI,($r = 0.441$, $p < 0.01$) for EVI calculated from Sentinel-2 imagery.

Table 4: Correlation between VIs and field estimation biomass for Landsat-8 and Sentinel-2

Vegetation Index	R		P-value	
	Sentinel-2	Landsat-8	Sentinel-2	Landsat-8
NDVI	0.797	0.708	<0.001	<0.001
DVI	0.455	0.380	<0.01	<0.01
SAVI	0.594	0.614	<0.001	<0.001
MSAVI	0.532	0.593	<0.001	<0.001
EVI	0.441	0.453	<0.01	<0.01
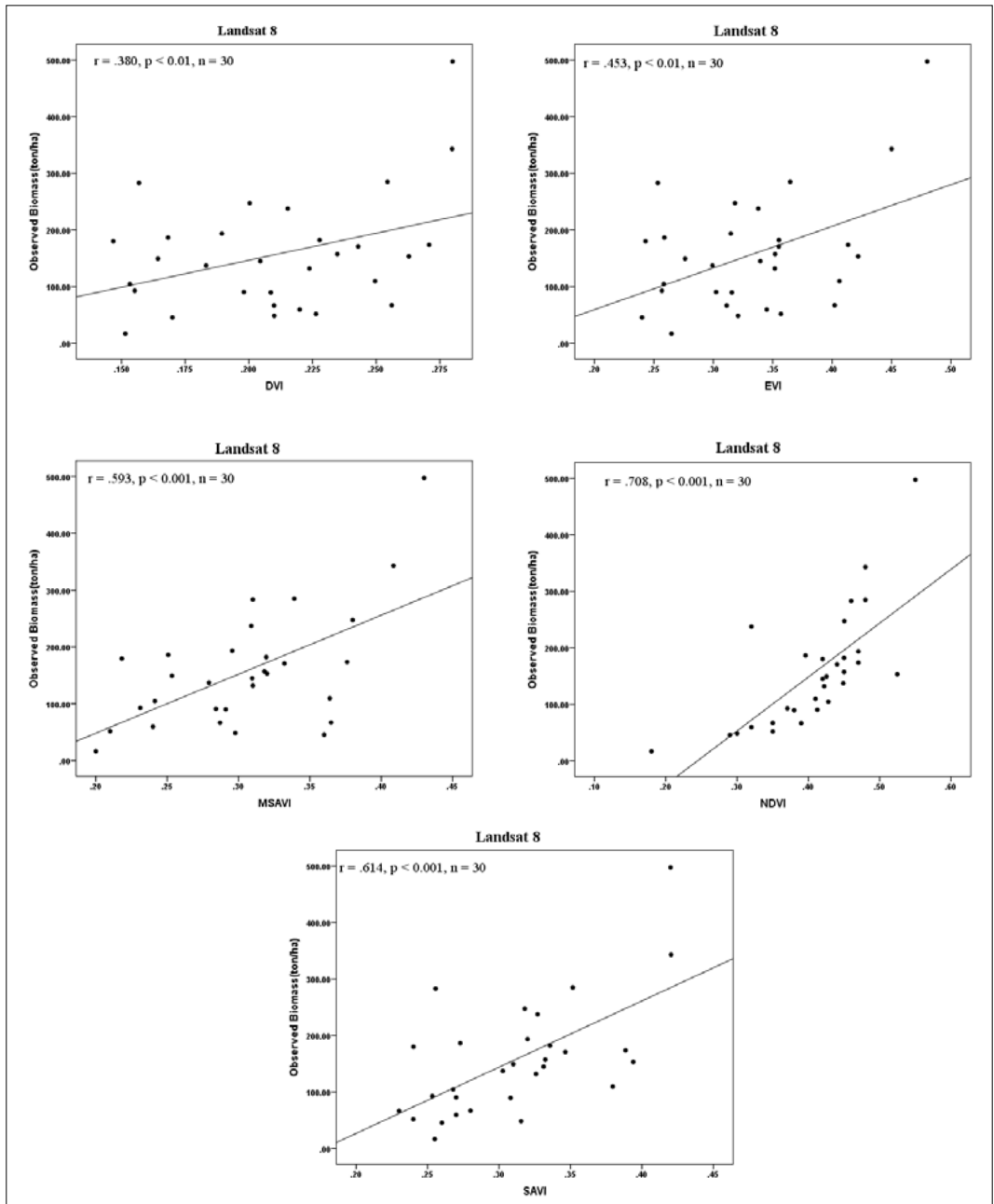
Figure 2: Scatterplots of correlation between the field estimated biomass and Landsat-8 VIs (NDVI, MSAVI, DVI, SAVI, EVI)
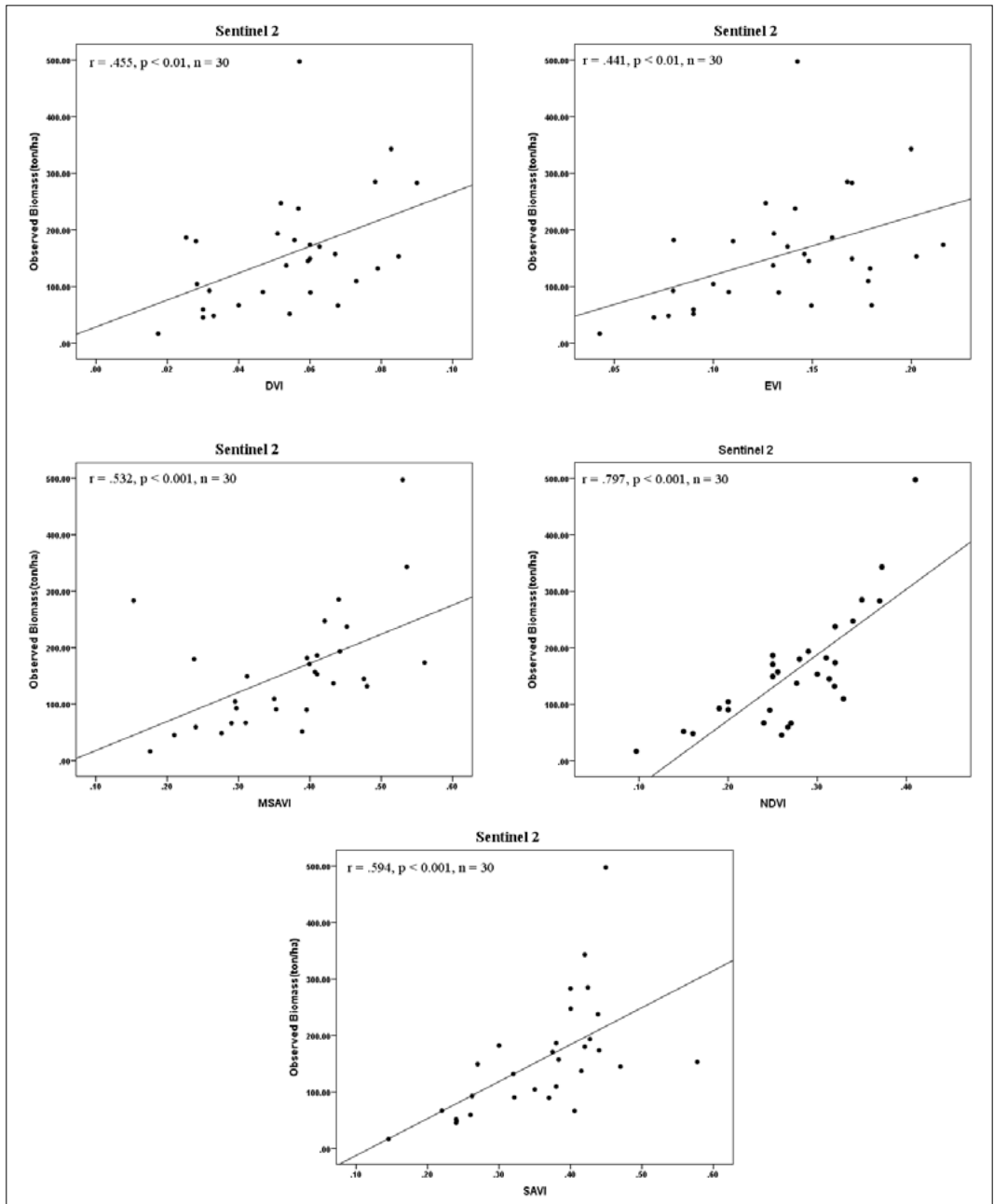
Figure 3: Scatter plots of correlation between the field estimated biomass and Sentinel-2 VIs (NDVI, MSAVI, DVI, SAVI, EVI)

Modelling the relationship between VIs and Field AGB

The established statistical models from simple linear regression analysis for biomass estimation between the VIs (NDVI, DVI, MSAVI, SAVI, and EVI) from both Landsat-8 and sentinel-2 and the biomass estimated from the field inventory showed moderate relationships. The established linear regression models and R^2 value of Landsat-8 and Sentinel-2 indices are summarized in Table 6 and Table 7 respectively and represented in scatter plot graphs in Figure 4 and Figure 5 respectively. Four Landsat-8 indices (NDVI, DVI, SAVI, and EVI) gave low values of R^2 as compared to the Sentinel-2 indices. However, one Landsat-8 index (MSAVI) obtained greater value of R^2 in comparison to the Sentinel-2 index. It is found that NDVI from Sentinel-2 obtained the highest value of R^2 (0.733),

followed by NDVI from Landsat-8 ($R^2 = 0.690$). Only the DVI vegetation index had a weak relationship with the field estimated biomass for both the satellites. Overall, the existing relationship between the VIs with field estimated biomass implies that they can be used to estimate biomass. However, only the NDVI-based models (Equation i and Equation vi) of both Landsat-8 and Sentinel-2 were used for further validation since they were found to be the best predictor of biomass among all other indices used.

The results of this study show a moderate performance, which could be due to the highly heterogeneous characteristics of a forest tree. For example, Wilkes et al. (2018) highlight the challenges of biomass estimation using remote sensing due to tree structure, heterogeneity, and complex land cover.

Table 5: Biomass estimation using simple linear regression model for Landsat-8 and Sentinel-2

Satellite	VegetationIndex	Model	R2	p-value	Equation
Landsat-8	NDVI	AGB = -355.66 + 1201.711*NDVI	0.690	<0.0001	i
	DVI	AGB = -86.097+ 1126.303*DVI	0.344	<0.001	ii
	SAVI	AGB = -183.389 + 1067.399*SAVI	0.527	<0.0001	iii
	MSAVI	AGB=-137.376+ 965.470*MSAVI	0.523	<0.0001	iv
	EVI	AGB = -138.777+ 863.058*EVI	0.405	<0.0001	v
Sentinel-2	NDVI	AGB = -113.602 + 983.414*NDVI	0.733	<0.0001	vi
	DVI	AGB = 17.712+ 2555.562*DVI	0.360	<0.001	vii
	SAVI	AGB = -120.683+ 771.947*SAVI	0.574	<0.0001	viii
	MSAVI	AGB = -59.256 + 547.585*MSAVI	0.456	<0.0001	ix
	EVI	AGB = -30.340 + 1314.922*EVI	0.483	<0.0001	x
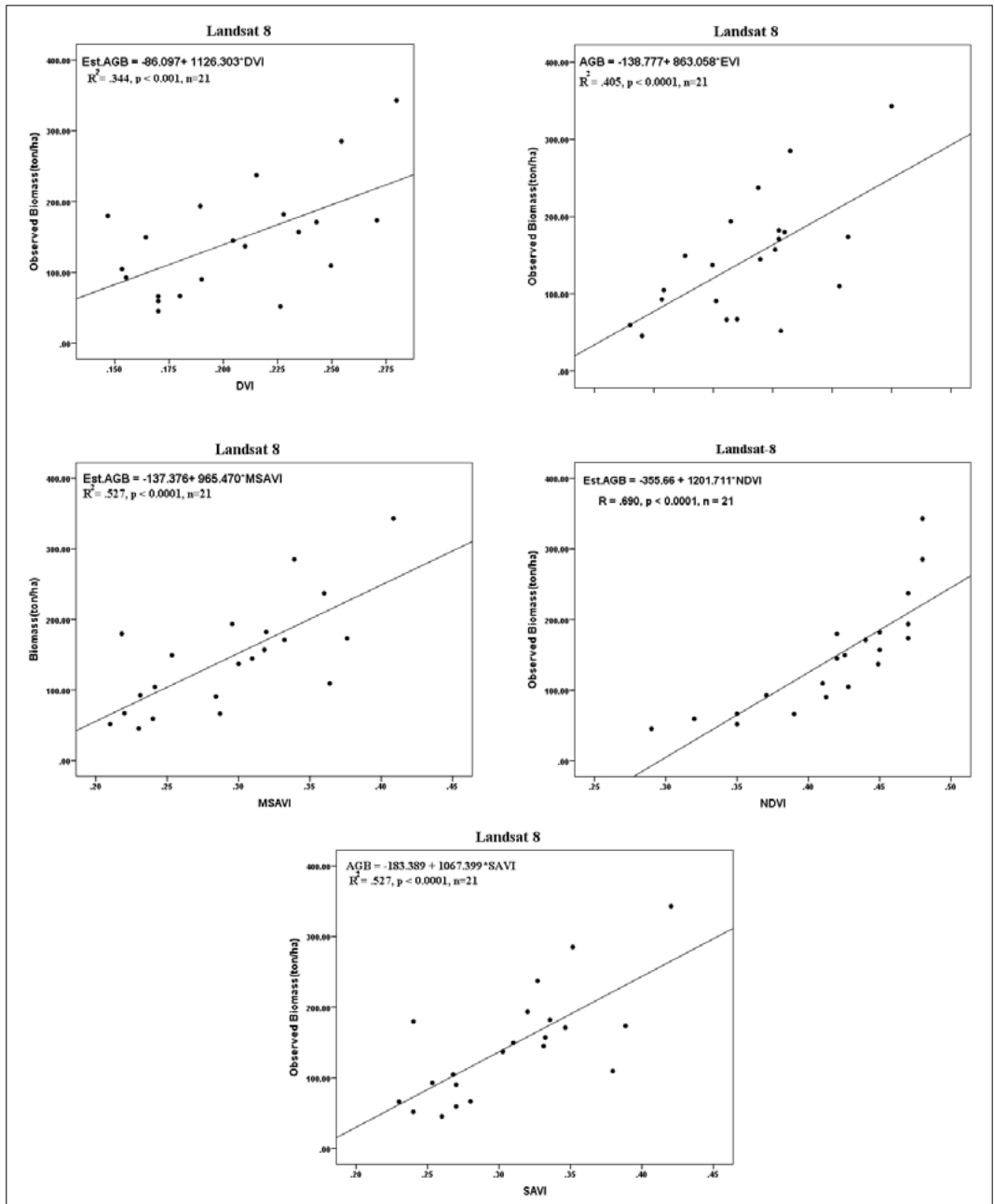
Figure 4: Scatterplots of Regression model for biomass estimate from Landsat-8 VIs(NDVI, MSAVI, DVI, SAVI, EVI)
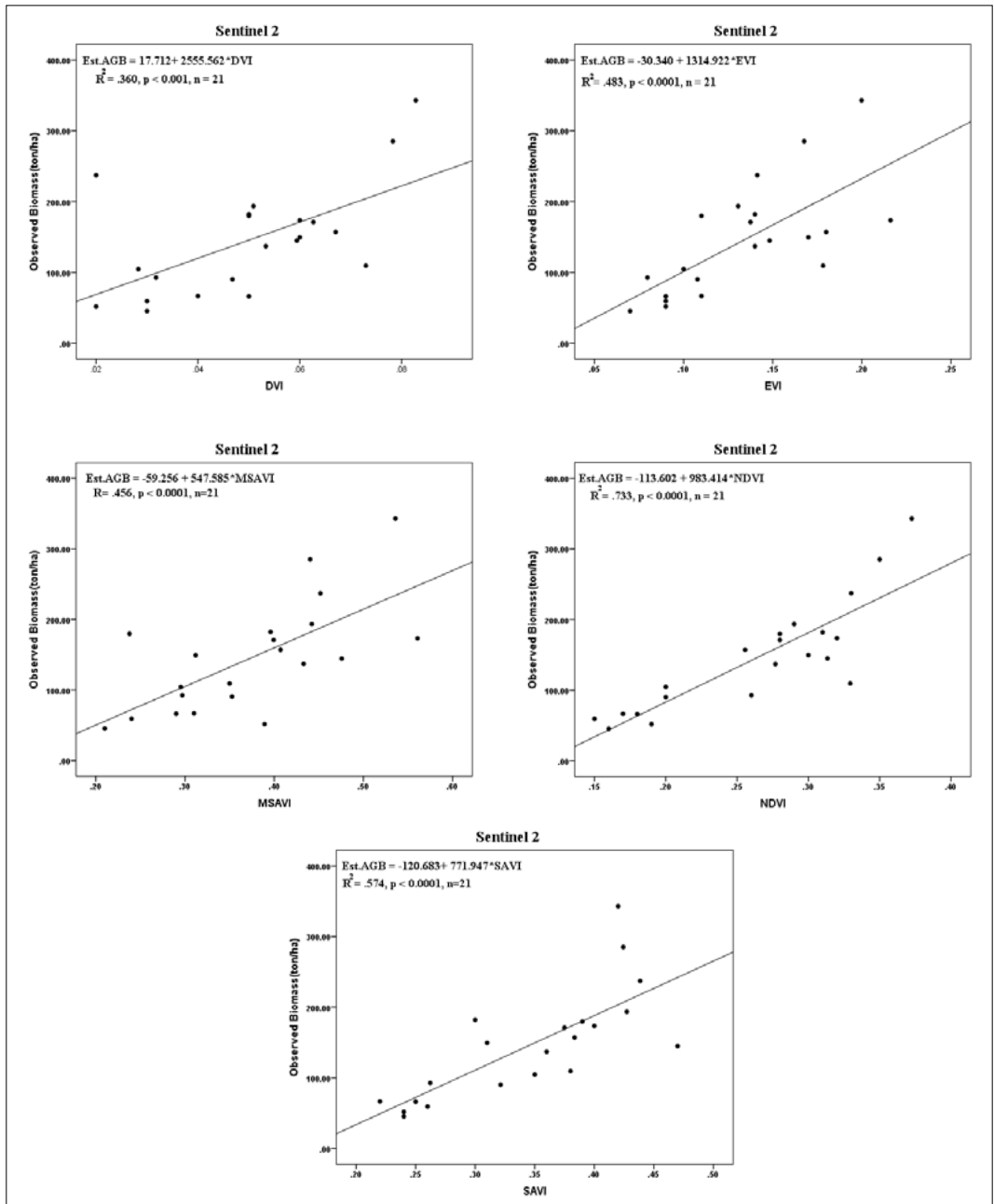
Figure 5: Scatterplots of regression model for biomass estimate from Sentinel-2 VIs (NDVI, MSAVI, DVI, SAVI, EVI)

Model validation and mapping of biomass and carbon stock

The assessment of model performance for estimating biomass using NDVI-based models (Equation i and Equation vi) showed good performance in both Landsat-8 and Sentinel-2 imagery. Comparison between Sentinel-2 and Landsat-8 (Figure 6 and Figure 7) showed that highest coefficient of determination (R^2) and least P-value was between predicted and observed biomass with the value of $R^2 = 0.76$ and $p < 0.001$ respectively. The lowest RMSE found was 78.44 ton ha^{-1} based on NDVI linear regression model (Equation vi) derived from Sentinel-2. It indicated that approximately 76% of the observed AGB was explained by the predicted AGB according to this model (Figure 6).

The biomass map and carbon stock map based on this model (Equation vi) is shown in Figure 8 and Figure 9 respectively, using the raster calculator in QGIS 3.8.2. The AGB values predicted from this model ranged from 0 to 402.31 ton ha^{-1} with the mean value of 129.82 ton ha^{-1}. Using the 0.47 conversion factor from IPCC (2006), the aboveground carbon (AGC) estimated from the study area was 61.01 ton ha^{-1}.

Many studies have indicated the successful application of optical remote sensing data such as Sentinel-2 and Landsat-8 for biomass estimation. For instance, Sibanda et al. (2015) compared Sentinel-2 MSI and Landsat 8 OLI estimations of the AGB of different vegetations. Their results showed better performance by Sentinel-2 derived models, with an R^2 value of 0.81 and an RMSE of prediction (RMSEP) value of 1.07 kg m^{-1}. Landsat 8 OLI yielded a slightly lower R^2 value of 0.76 and an RMSEP value of 1.15 kg m^{-1}. The findings of this study are similar to this result. Furthermore, the sample plots of this study were constrained by accessibility, time and cost. Nevertheless, the sample plots were successful in establishing a model ($R^2 = 0.76$) and predicted AGB map on the study area. The reason why the model on this research shows good performance might be that the forest being moderately dense as Anaya et al. (2009) reported that optical remote sensing-based biomass estimation performs better at low biomass levels . The same has also been reported by Kushwaha et al. (2014) and Manna et al. (2014).

The results of this study provide useful information to managers and planners and can be used as a valuable input in devising working/ management plans and prioritizing areas for conservation.
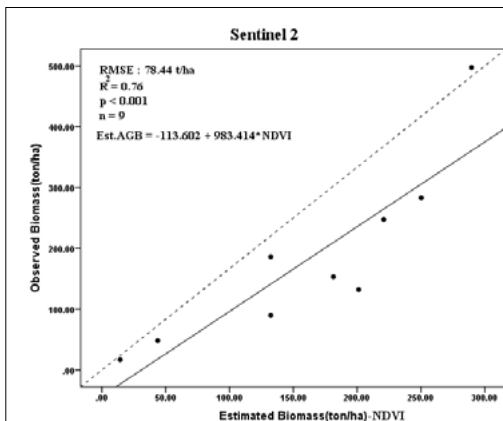
Figure 6: Scatterplot of assessment of model performance for biomass estimation (validation) for Sentinel-2 NDVI
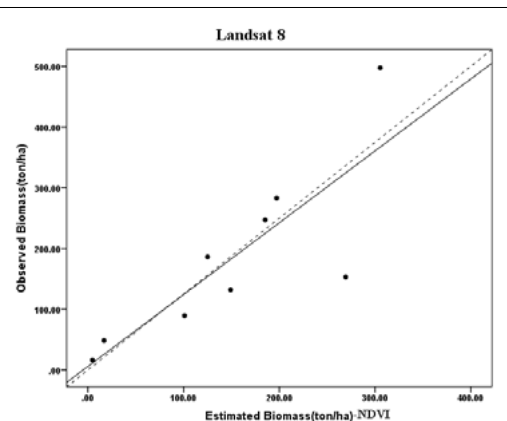
Figure 7: Scatterplot of assessment of model performance for biomass estimation (validation) for Landsat-8 NDVI
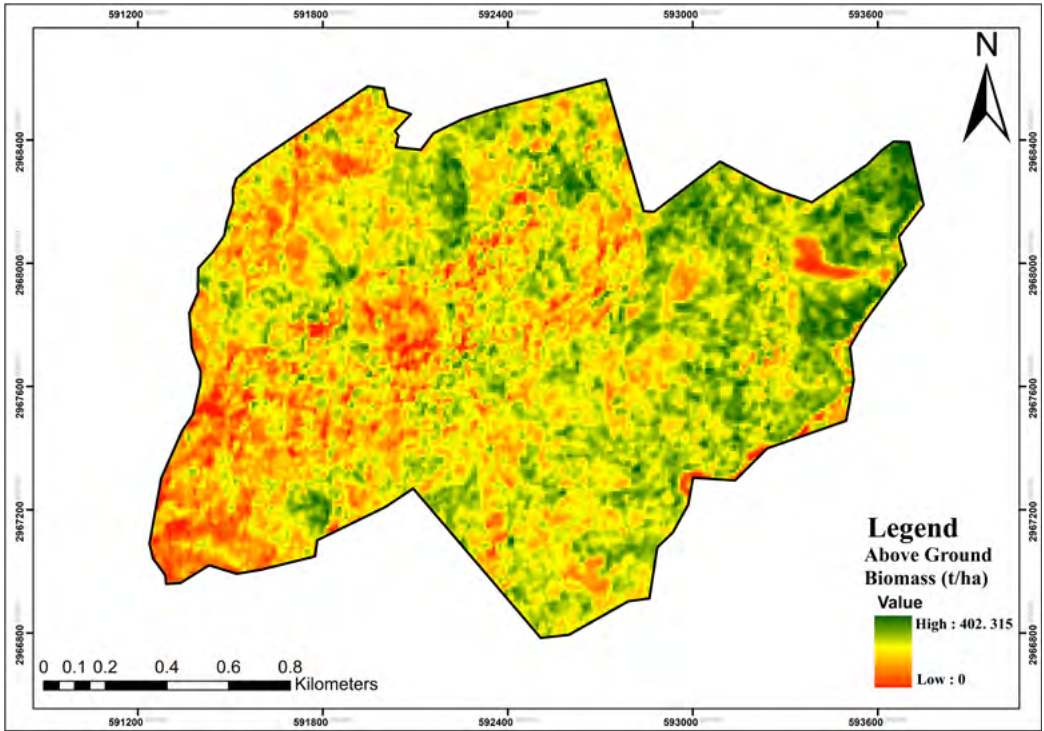
Figure 8: Biomass distribution Map predicted from Sentinel-2 NDVI
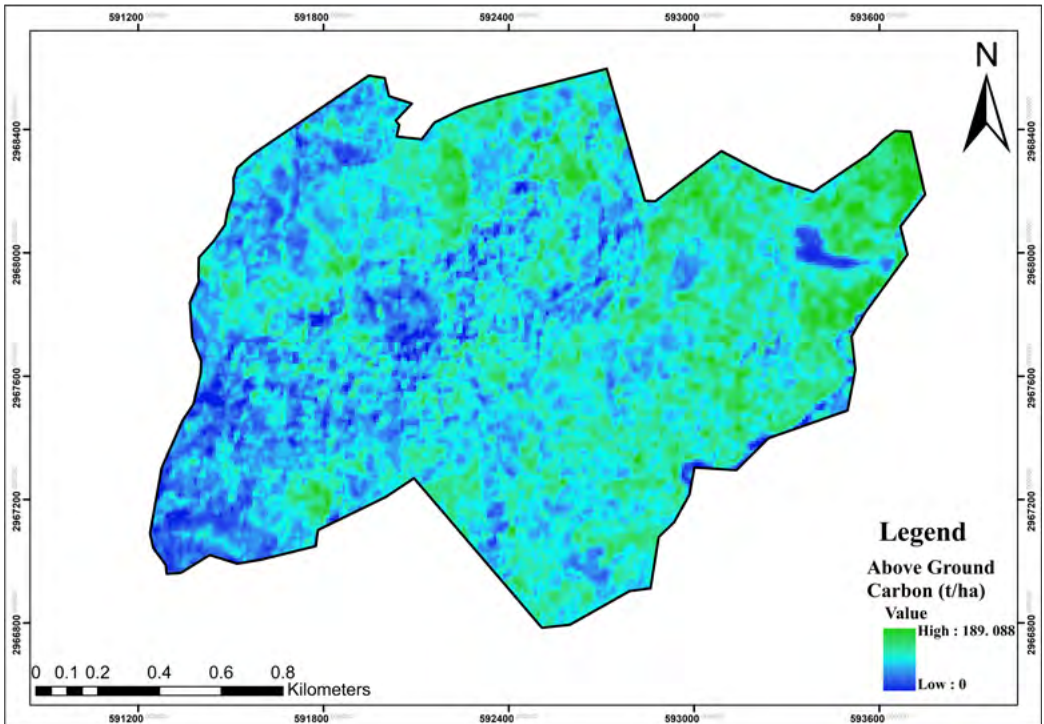
Figure 9: Carbon stock distribution Map predicted from Sentinel-2 NDVI

Conclusion and Recommendation

A remote sensing-based model for AGB retrieval in a community forest setting was developed from VIs (SAVI, NDVI, DVI, MSAVI, and EVI) derived from Sentinel-2 and Landsat-8 data sets as well as field data extracted from 30 plots. Comparison between Sentinel-2 and Landsat-8 showed that regression equation linear modelling based on NDVI data derived from Sentinel-2 was found to be the better model for predicting biomass. It indicated that approximately 76% of the observed AGB was explained by the predicted AGB according to this model and was the best fitted model. Despite good estimates of the AGB in this study, our models are limited to the study area due to small number of field plots data. Future studies should increase the number of field plots as regression models often perform best when established on a much larger sample and hence can generalize for greater area.

The study suggested that Sentinel-2 product has the greater potential to estimate biomass and map forest areas. This may be due to its higher resolution than that of the Landsat-8. It also shows that the SalboteKarele community forest is of considerable significance as it stores suitable amounts of carbon despite disturbance from anthropogenic factor in some areas. Thus, the study assessed the value of these forests in terms of carbon sequestration, demonstrating that there is a significant potential for CO_2 sequestration, as well as their environmental role in combating climate change. As a result, it is concluded that, by growing and protecting these forests, a significant amount of carbon can be sequestered in the future. As a result, additional carbon credits can be obtained through carbon trading in the context of REDD+ forest management.

Acknowledgements

References

Ali, I., Cawkwell, F., Green, S., & Dwyer, N. (2014). Application of statistical and machine learning models for grassland yield estimation based on a hypertemporal satellite remote sensing time series. *Geoscience and remote sensing symposium* (pp. 5060-5063). IEEE.

Anaya, J. A., Chuvieco, E., & Palacios-Orueta, A. (2009). Aboveground biomass assessment in Colombia: A remote sensing approach. *Forest Ecology and Management*, *257*(4), 1237-1246.

Asner, G. P. (2009). Tropical forest carbon assessment: integrating satellite and airborne mapping approaches. *Environmental Research Letters*, *4*(3), 034009.

Atzberger, C., & Richter, K. (2012). Spatially constrained inversion of radiative transfer models for improved LAI mapping from future Sentinel-2 imagery. *Remote Sensing of Environment*, *120*, 208-218.

Barati, S., Rayegani, B., Saati, M., Sharifi, A., & Nasri, M. (2011). Comparison the accuracies of different spectral indices for estimation of vegetation cover fraction in sparse vegetated areas. *The Egyptian Journal of Remote Sensing and Space Science*, *14*(1), 49–56. https://doi.org/10.1016/J.EJRS.2011.06.001

Bhattarai, K. / O. ; R., Bhattarai, K. R., & Khadka, M. K. (2016). Ethnobotanical survey of medicinal plants from Ilam District, East Nepal. *Nepjol.Info*, *14*(1), 78–91. https://doi.org/10.3126/on.v14i1.16444

Chave, J., Réjou-Méchain, M., Búrquez, A., Chidumayo, E., Colgan, M. S., Delitti, W. B. C., Duque, A., Eid, T., Fearnside, P. M., Goodman, R. C., Henry, M., Martínez-Yrízar, A., Mugasha, W. A., Muller-Landau, H. C., Mencuccini, M., Nelson, B. W., Ngomanda, A., Nogueira, E. M., Ortiz-Malavassi, E., … Vieilledent, G. (2014). Improved allometric models to estimate the aboveground biomass of tropical trees. *Global Change Biology*, *20*(10), 3177–3190. https://doi.org/10.1111/GCB.12629

Chavez Jr, P. S. (1988): An improved dark-object subtraction technique for atmospheric scattering correction of multispectral data. – Remote sensing of environment 24: 459-479.

Chinembiri, T. S., Bronsveld, M. C., Rossiter, D. G., & Dube, T. (2013). The precision of C stock estimation in the Ludhikola watershed using model-based and design-based

approaches. *Natural resources research*, *22*, 297-309.

Clevers, J. G., & Gitelson, A. A. (2013). Remote estimation of crop and grass chlorophyll and nitrogen content using red-edge bands on Sentinel-2 and-3. *International Journal of Applied Earth Observation and Geoinformation*, *23*, 344-351.

Delegido, J., Verrelst, J., Alonso, L., & Moreno, J. (2011). Evaluation of sentinel-2 red-edge bands for empirical estimation of green LAI and chlorophyll content. *Sensors*, *11*(7), 7063-7081.

Dube, T., & Mutanga, O. (2015). Evaluating the utility of the medium-spatial resolution Landsat 8 multispectral sensor in quantifying aboveground biomass in uMgeni catchment, South Africa. *ISPRS Journal of Photogrammetry and Remote Sensing*, *101*, 36-46.

FAO (2010) Global Forest Resource Assessment (FRA). FAO forestry paper 163. Food and Agriculture Organization (FAO) of the United Nations Rome.

Frampton, W. J., Dash, J., Watmough, G., & Milton, E. J. (2013). Evaluating the capabilities of Sentinel-2 for quantitative estimation of biophysical variables in vegetation. *ISPRS journal of photogrammetry and remote sensing*, *82*, 83-92.

FRTC. (2022). *National Land Cover Monitoring System of Nepal*. https://frtc.gov.np/uploads/files/3053_GoN_National land cover monitoring system for Nepal - 18 April 2022_WEB.pdf

Gara, T. W., Murwira, A., Chivhenge, E., Dube, T., & Bangira, T. (2014). Estimating wood volume from canopy area in deciduous woodlands of Zimbabwe. *Southern Forests: A Journal of Forest Science*, *76*(4), 237-244.

Godinho, S.; Guiomar, N.; Gil, A. (2017). Estimating tree canopy percentage in Mediterranean slivopastoral systems in suing Sentinel-2A imagery and the stochastic gradient boosting algorithm. Int. J. Remote Sens., 1–23.

Hall, R. J., Skakun, R. S., Arsenault, E. J., & Case, B. S. (2006). Modeling forest stand structure attributes using Landsat ETM+ data: Application to mapping of aboveground biomass and stand volume. *Forest ecology and management*, *225*(1-3), 378-390.

Henry, M., Picard, N., Trotta, C., Manlay, R., Valentini, R., Bernoux, M., Saint-André, L., Manlay, R. J., Henry, L. S.-A., Picard,

M., Trotta, N., Valentini, R. J., & Bernoux, R. (2011). Estimating tree biomass of sub-Saharan African forests: a review of available allometric equations. *Hal.Inrae.Fr*, *45*(3), 477–569. https://hal.inrae.fr/hal-02651041

Herold, M., & Johns, T. (2007). Linking requirements with capabilities for deforestation monitoring in the context of the UNFCCC-REDD process. *Environmental Research Letters*, *2*(4), 045025.

Husch, B., Beers, T., & Kershaw Jr, J. (2003). Forest Mensuration, ; John willey & Sons. *Inc.: Hoboken, NJ, USA*, 443.

Hussin, Y. A., & Gilani, H. (2011). Mapping carbon stocks in community forests of Nepal using high spatial resolution satellite images. *Sustainable Mountain Development*, *60*, 22-24.

Journal, P., Joshi, M., Srivastava, R. K., Vahlne, N., Ahlgren, E. O., Bruce, N., Perez-Padilla, R., Albalak, R., Ipcc, US EPACenter for Corporate Climate Leadership, O. a R., Herold, A., Saxena, N. C., Habermehl, H., Fao, Jeuland, M. A., Pattanayak, S. K., Fuels, C., Garg, A., Mohan, P., … Helena, S. (2006). 2006 IPCC Guidelines for National Greenhouse Gas Inventories. *Genebra, Suíça*, *66*(4), 44. https://doi.org/10.1209/epl/i2005-10515-2

Kaplan, G., & Avdan, U. (2017). Mapping and monitoring wetlands using Sentinel-2 satellite imagery.

Kasischke, E.S.; Goetz, S.; Hansen, M.C.; Ozdogan, M.; Rogan, J.; Ustin, S.L.; Woodcock, C.E. (2014) Remote Sensing for Natural Resource Management and Environmental Monitoring, 3rd ed.; John and Wiley and Sons, Inc.: Hoboken, NJ, USA.

Kim, S. R., Kwak, D. A., oLee, W. K., Son, Y., Bae, S. W., Kim, C., & Yoo, S. (2010). Estimation of carbon storage based on individual tree detection in Pinus densiflora stands using a fusion of aerial photography and LiDAR data. *Science China Life Sciences 2010 53:7*, *53*(7), 885–897. https://doi.org/10.1007/S11427-010-4017-1

Kushwaha, S. P. S., Nandy, S., & Gupta, M. (2014). Growing stock and woody biomass assessment in Asola-Bhatti Wildlife Sanctuary, Delhi, India. *Environmental Monitoring and Assessment*, *186*(9), 5911–5920. https://doi.org/10.1007/S10661-014-3828-0

Lu, D. (2005). Aboveground biomass estimation

using Landsat TM data in the Brazilian Amazon. *International journal of remote sensing*, *26*(12), 2509-2525.

Lu, D. (2006). The potential and challenge of remote sensing-based biomass estimation. *International journal of remote sensing*, *27*(7), 1297-1328.

Lu, D., Chen, Q., Wang, G., Moran, E., Batistella, M., Zhang, M., ... & Saah, D. (2012). Aboveground forest biomass estimation with Landsat and LiDAR data and uncertainty analysis of the estimates. *International Journal of Forestry Research*, *2012*.

Majasalmi, T., & Rautiainen, M. (2016). The potential of Sentinel-2 data for estimating biophysical variables in a boreal forest: A simulation study. *Remote Sensing Letters*, *7*(5), 427–436. https://doi.org/10.1080/2150 704X.2016.1149251

Manna, S., Nandy, S., Chanda, A., Akhand, A., Hazra, S., & Dadhwal, V. K. (2014). Estimating aboveground biomass in Avicennia marina plantation in Indian Sundarbans using high-resolution satellite data. *Spiedigitallibrary. Org*. https://doi.org/10.1117/1.JRS.8.083638

Naesset, E., Ørka, H. O., Solberg, S., Bollandsås, O. M., Hansen, E. H., Mauya, E., ... & Gobakken, T. (2016). Mapping and estimating forest area and aboveground biomass in miombo woodlands in Tanzania using data from airborne laser scanning, TanDEM-X, RapidEye, and global forest maps: A comparison of estimated precision. *Remote sensing of Environment*, *175*, 282-300.

Nepal, F. R. A. (2015). State of Nepal's forests. *Forest Resource Assessment (FRA)*.

Palareti, G., Legnani, C., Cosmi, B., Antonucci, E., Erba, N., Poli, D., Testa, S., & Tosetto, A. (2016). Comparison between different D-Dimer cutoff values to assess the individual risk of recurrent venous thromboembolism: Analysis of results obtained in the DULCIS study. *International Journal of Laboratory Hematology*, *38*(1), 42–49. https://doi. org/10.1111/ijlh.12426

Piñeiro, G., Perelman, S., Guerschman, J. P., & Paruelo, J. M. (2008). How to evaluate models: Observed vs. predicted or predicted vs. observed? *Ecological Modelling*, *216*(3–4), 316–322. https://doi.org/10.1016/J. ECOLMODEL.2008.05.006

Powell, S. L., Cohen, W. B., Healey, S. P., Kennedy, R. E., Moisen, G. G., Pierce, K. B., & Ohmann, J. L. (2010). Quantification of live aboveground forest biomass dynamics with Landsat time-series and field inventory data: A comparison of empirical modeling approaches. *Remote Sensing of Environment*, *114*(5), 1053-1068.

Ramoelo, A., Cho, M., Mathieu, R., & Skidmore, A. K. (2015). Potential of Sentinel-2 spectral configuration to assess rangeland quality. *Journal of applied remote sensing*, *9*(1), 094096-094096.

Rozendaal, D. M. A., Requena Suarez, D., De Sy, V., Avitabile, V., Carter, S., Adou Yao, C. Y., Alvarez-Davila, E., Anderson-Teixeira, K., Araujo-Murakami, A., Arroyo, L., Barca, B., Baker, T. R., Birigazzi, L., Bongers, F., Branthomme, A., Brienen, R. J. W., Carreiras, J. o. M. B., Cazzolla Gatti, R., Cook-Patton, S. C., ... Herold, M. (2022). Aboveground forest biomass varies across continents, ecological zones and successional stages: Refined IPCC default values for tropical and subtropical forests. *Environmental Research Letters*, *17*(1). https://doi.org/10.1088/1748-9326/ac45b3

Sibanda, M., Mutanga, O., & Rouget, M. (2015). Examining the potential of Sentinel-2 MSI spectral resolution in quantifying above ground biomass across different fertilizer treatments. *ISPRS Journal of Photogrammetry and Remote Sensing*, *110*, 55-65.

Subedi, B., Lamichhane, P., Magar, L. K., & Subedi, T. (2022). *Aboveground carbon stocks and sequestration rates of forests under different management regimes in Churia region of Nepal. 32*(1), 15–24.

Vashum, K. T., & Jayakumar, S. (2012). Methods to estimate above-ground biomass and carbon stock in natural forests-a review. *Journal of Ecosystem & Ecography*, *2*(4), 1-7.

Viana, H., Aranha, J., Lopes, D., & Cohen, W. B. (2012). Estimation of crown biomass of Pinus pinaster stands and shrubland above-ground biomass using forest inventory data, remotely sensed imagery and spatial prediction models. *Ecological Modelling*, *226*, 22-35.

Wilkes, P., Disney, M., Vicari, M. B., Calders, K., & Burt, A. (2018). Estimating urban above ground biomass with multi-scale LiDAR. *Carbon Balance and Management*, *13*(1). https://doi.org/10.1186/S13021-018-0098-0